



**Report 315**

*July 2017*

# The Future Water Risks Under Global Change in Southern and Eastern Asia: Implications of Mitigation

Xiang Gao, C. Adam Schlosser, Charles Fant and Kenneth Strzepek

**MIT Joint Program on the Science and Policy of Global Change** combines cutting-edge scientific research with independent policy analysis to provide a solid foundation for the public and private decisions needed to mitigate and adapt to unavoidable global environmental changes. Being data-driven, the Joint Program uses extensive Earth system and economic data and models to produce quantitative analysis and predictions of the risks of climate change and the challenges of limiting human influence on the environment—essential knowledge for the international dialogue toward a global response to climate change.

To this end, the Joint Program brings together an interdisciplinary group from two established MIT research centers: the **Center for Global Change Science (CGCS)** and the **Center for Energy and Environmental Policy Research (CEEPR)**. These two centers—along with collaborators from the Marine Biology Laboratory (MBL) at

Woods Hole and short- and long-term visitors—provide the united vision needed to solve global challenges.

At the heart of much of the program's work lies MIT's Integrated Global System Model. Through this integrated model, the program seeks to discover new interactions among natural and human climate system components; objectively assess uncertainty in economic and climate projections; critically and quantitatively analyze environmental management and policy proposals; understand complex connections among the many forces that will shape our future; and improve methods to model, monitor and verify greenhouse gas emissions and climatic impacts.

This reprint is intended to communicate research results and improve public understanding of global environment and energy challenges, thereby contributing to informed debate about climate change and the economic and social implications of policy alternatives.

*—Ronald G. Prinn and John M. Reilly,  
Joint Program Co-Directors*

# The Future Water Risks Under Global Change in Southern and Eastern Asia: Implications of Mitigation

Xiang Gao<sup>1,2</sup>, C. Adam Schlosser<sup>1</sup>, Charles Fant<sup>3</sup> and Kenneth Strzepek<sup>1</sup>

**Abstract:** Understanding and predicting the future vulnerability of freshwater resources is a major challenge with important societal implications. Many studies have identified Asia as a hotspot of severe water stress in the coming decades, and also highlighted the large uncertainty associated with water resource assessment based on limited multi-model projections. Here we provide a more comprehensive risk-based assessment of water use and availability in response to future climate change, socioeconomic growth, and their combination in Southern and Eastern Asia. We employ a large ensemble of scenarios that capture the spectrum of regional climate response as well as a range of economic projections and climate policies in a consistent, integrated modeling framework. We show that economic growth increases water stress ubiquitously. The climate-only and combined climate-growth effects on water stress remain largely negative in China and Indus Basin, but largely positive in India, Indochina, and Ganges Basin. However, climate poses substantially large uncertainty in water stress changes than socioeconomic growth. By 2050, socioeconomic growth alone can lead to an additional 650 million people living under at least “heavy” water stress, with most of these located in India, Indus Basin, and China. The combined effects of socioeconomic growth and climate change reduce people under water stress to an additional 200 million, attributed mainly to the beneficial climate in India that moves its heavily-stressed condition into the slightly or moderately-stressed conditions. These 200 million people primarily reside in Indus Basin and China under at least overly exploited water conditions—where total water requirements will consistently exceed surface water supply. Climate mitigation helps alleviating the risks of increasing water scarcity by midcentury, but to a limited extent. Therefore, adaptive measures need to be taken to meet these surface water shortfalls, or a combination of both approaches may be most effective.

1. INTRODUCTION .....	2
2. MODELS AND METHODS .....	2
3. RESULTS .....	3
3.1 WATER STRESS INDEX .....	3
3.2 POPULATION AT RISK TO WATER STRESS .....	9
4. SUMMARY AND DISCUSSION .....	11
5. REFERENCES .....	12

1 Joint Program on the Science and Policy of Global Change, Massachusetts Institute of Technology, MA, USA

2 Corresponding author (Email: [xgao304@mit.edu](mailto:xgao304@mit.edu)).

3 Industrial Economics, Inc., Cambridge, MA, USA

## 1. Introduction

Water, the most vital of all resources, is essential for socio-economic development and maintaining healthy ecosystems. Yet, water scarcity now affects more than two-fifths of the people on Earth, and by 2025 two-thirds of the global population is likely to be living under water-stressed conditions (UN-Water, 2007). In addition, the majority of the world's people living in water-related despair will be in Asia (Chellaney, 2012). Asia is home to 60% of the global population (Population Reference Bureau, 2015), yet is the world's driest continent with availability of freshwater less than half the global annual average of 6,380 m<sup>3</sup> per inhabitant (Chellaney, 2012). In the face of rapidly rising populations, the fastest-growing economy, expanding irrigation and water-intensive industries, and spiraling household consumption, per capita water availability in Asia is declining by 1.6% per year (Chellaney, 2012). Climate change will further exacerbate existing water scarcity in Asia via altering the hydrological cycle, such as changing rainfall patterns, increasing the variability and frequency of extreme events (flooding and drought), and reducing the availability of renewable resources (glaciers and rivers, etc.) (Siegfried *et al.*, 2011). For decades to come, the spreading water stress in Asia will have direct consequences for economic and human development as well as environmental sustainability.

Understanding the vulnerability of freshwater resources in Asia is therefore vital to ensuring sustainable water management in the region. However, the future adequacy of freshwater resources is difficult to assess, owing to a complex and rapidly changing geography of water supply and consumption as a result of multifaceted interplay among human society, terrestrial hydrological cycles and climate change (Arnell, 2004; Alcamo *et al.*, 2007;

Haddeland *et al.*, 2014; Hagemann *et al.*, 2013). Previous studies used single (Arnell, 2004; Alcamo *et al.*, 2007; Vörösmarty *et al.*, 2000) or several (Haddeland *et al.*, 2014; Schewe *et al.*, 2014; Hagemann *et al.*, 2013) global hydrological models forced with multiple climate model projections to examine the vulnerability of global water resources from climate change and/or direct human impacts. These studies highlighted a large uncertainty associated with projected changes in water resources within such climate-hydrology modelling chains. However, the limited ensembles employed in these studies only allow for the quantification of such uncertainty with a multi-model ensemble spread. Here we focus on a more comprehensive risk-based assessment of water use and availability as well as water resource adequacy in response to future climate change, socioeconomic growth, and their combination in large watersheds—or Assessment Sub-Regions (ASRs)—in Southern and Eastern Asia, which have been documented in previous studies as hotspots of the severe water stress in the future (Arnell, 2004; Alcamo *et al.*, 2007; Haddeland *et al.*, 2014; Schlosser *et al.*, 2014). In particular, we focus on major political regions (China, India, and the Indo-Chinese peninsula or Indochina) and several basins (Indus, Ganges, and Brahmaputra) (**Figure 1**).

## 2. Models and Methods

Aggregated mean annual surface runoff within each ASR and inflow of upstream ASRs constitute the water supply to which local human society has access. We consider the irrigated agriculture as well as the domestic and industrial sectors for water demands on a mean annual basis. Each component determines the degree to which humans interact with sustainable water supply and pro-

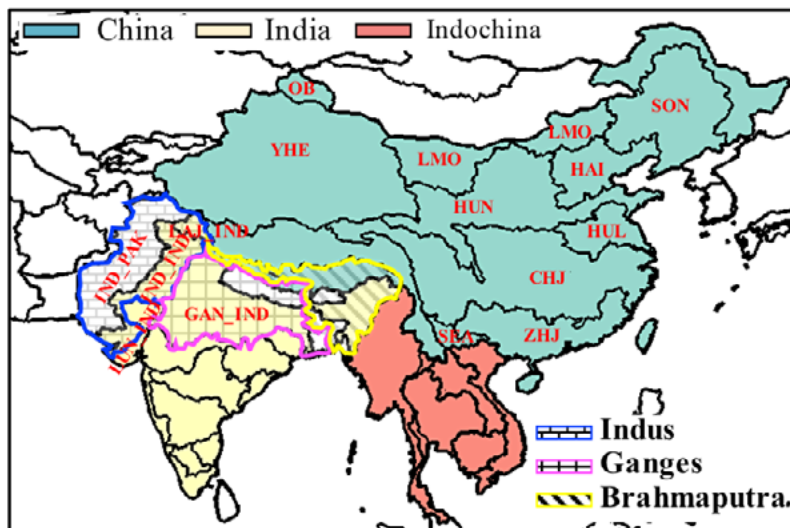


**Figure 1.** Maps of major political regions and basins in this study.

vides a local water stress index (WSI), defined as the ratio of water withdrawal to supply. This metric measures the pressure that human water uses exert on renewable surface water. Values on the order of 0.3 to 0.6 and 0.6 to 1.0 indicate medium to high stress, whereas those greater than 1.0 and 2.0 reflect conditions of severe and extreme water limitation, respectively (Smakhtin *et al.*, 2005). We consider vulnerability with respect to sustainable water resources only, under different levels of global warming, allowing for impact of climate change mitigation to be assessed. We do not explicitly model the policy response or long-term investment adaptation to climate change or development pressure.

We employ a water resource system (WRS) component embedded within the Massachusetts Institute of Technology Integrated Global System Model (IGSM) framework in a large ensemble of 50-year (2001–2050) simulations at  $2 \times 2.5^\circ$ —consistent across a range of climate policies, regional hydroclimate changes, climate parameters, and emissions of all greenhouse gases, aerosol, and pollutants. Most previous model-based studies, however, have been driven with exogenous climate forcing that is disconnected from consistent socioeconomic pathways, thus lacking the interactions between natural processes and human activities. We consider two greenhouse gas control policies: one with unconstrained emissions (UE) and the other imposing a 660 ppm CO<sub>2</sub>-equivalent stabilization target (L2S). For each policy scenario, we employ a 400-member ensemble of IGSM projections with different values of climate and economic parameters (Webster *et al.*, 2012), complemented with the pattern-scaling (Schlosser *et al.*, 2012) based on 17 climate models in the Coupled Model Intercomparison Project Phases 3 (CMIP3) (Meehl *et al.*, 2007) (**Figure 2**), to develop a 6,800-member ensemble of climate change projections. Gaussian Quadrature procedure (Arndt *et al.*, 2015) is then employed to produce a subset and respective weights that represent the full ensemble (539 and 630 members for UE and L2S, respectively). Contemporary climate is based on a 3-hourly, 1° global near-surface meteorology dataset (Sheffield *et al.*, 2006), but is detrended and adjusted to the year-2000 mean. Future atmospheric forcing is obtained with a delta method (Ramirez-Villegas and Jarvis, 2010) that incorporates the downscaled changes in climate from IGSM (anomalies with respect to 1981–2000 climatology) but maintains contemporary inter-annual climate variability. The runoff is simulated by the Community Land Model (CLM) (Oleson *et al.*, 2004) within the IGSM and bias corrected with a modification of the Maintenance of Variance Extension (MOVE) procedure (Strzepek *et al.*, 2013) such that each ASR contains as realistic natural flow conditions as possible.

Domestic and industrial demands are determined by projections of population and Gross Domestic Product (GDP) from the Economic Projection and Policy Analysis (EPPA) model (Paltsev, *et al.* 2004) within the IGSM. Future population at the ASR level is obtained by applying the constant growth rate to the contemporary population (Rosegrant *et al.*, 2008). Irrigation demand mainly responds to the climate (precipitation and temperature) and is calculated for a variety of crops with a crop water deficit module (CliCrop) (Fant *et al.*, 2012) of the WRS. The irrigated area is assumed constant at current estimates from IFPRI and irrigation efficiency is also fixed. The Water System Management (WSM) of the WRS optimizes the routing of water supply across all of the ASRs, which sets priority for domestic and industrial uses followed by the agriculture sector.

For each policy scenario, we formulate three impact scenarios to quantify the separate and combined contributions of climate change and socioeconomic growth to the degree of water stress out to 2050. The *Growth* scenario (“G”), where the socioeconomic growth alone influences water conditions with the domestic and industrial demands as key drivers, applies projected GDP and population with climate held at the contemporary condition. The same population projection is employed for both UE and L2S scenarios. The *Climate* scenario (“C”), where irrigation demand and runoff serve as the main drivers of water stress, varies climate but fixes the population and GDP at year 2000 levels. The *Climate and Growth* scenario (“CG”) imposes both climate change and socio-economic growth to assess the combined effects on water stress. We gauge the changes in water supply, demands, and water stress from these scenarios against a baseline scenario which represents a 50-year (2001–2050) simulation forced with contemporary climate and initial conditions at 2001 from the CLM run of 1948 to 2000 driven by near-surface meteorology dataset (Sheffield *et al.*, 2006). The baseline scenario produces 50-year runoff and irrigation demand with the domestic and industrial demands held constant at the values of year-2000. We further assess the uncertainty of baseline water stress from internal climate variability with a 500-member ensemble by performing a multivariate k-nearest neighbor bootstrap (Lall and Sharma, 1996). We focus our analyses of these metrics on their distributions of relative decadal mean changes (2041–2050) from the baseline of the same period, so the interannual or seasonal variations have not been specifically studied here.

### 3. Results

#### 3.1 Water Stress Index

**Figure 3** presents the relative changes in WSI over the major political regions and basins, weighted by the

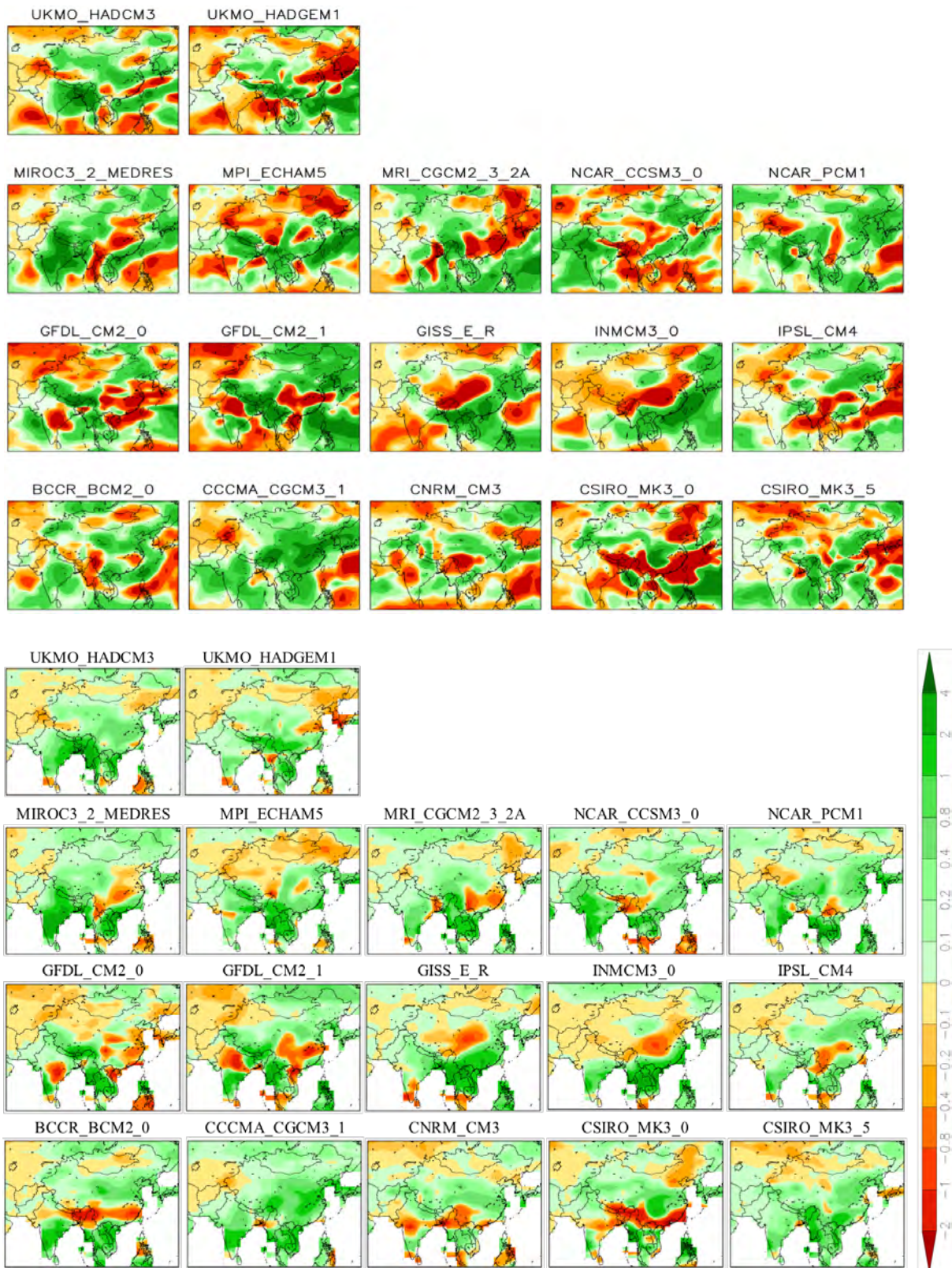


**Figure 2.** Top panel: Shifts in pattern-scaling transformation coefficients with respect to global temperature change  $dC_{x,y}/dT_{\text{Global}}$  ( $K^{-1}$ ) for June precipitation based on the CMIP3 climate models. Bottom panel: Changes in decadal averaged June precipitation (with decadal average changes from the baseline run removed) between 2041-2050 and 2001-2010 (mm/day). The spatial patterns of the CMIP3 climate models (top panel) are well preserved in the corresponding precipitation changes (Bottom panel).

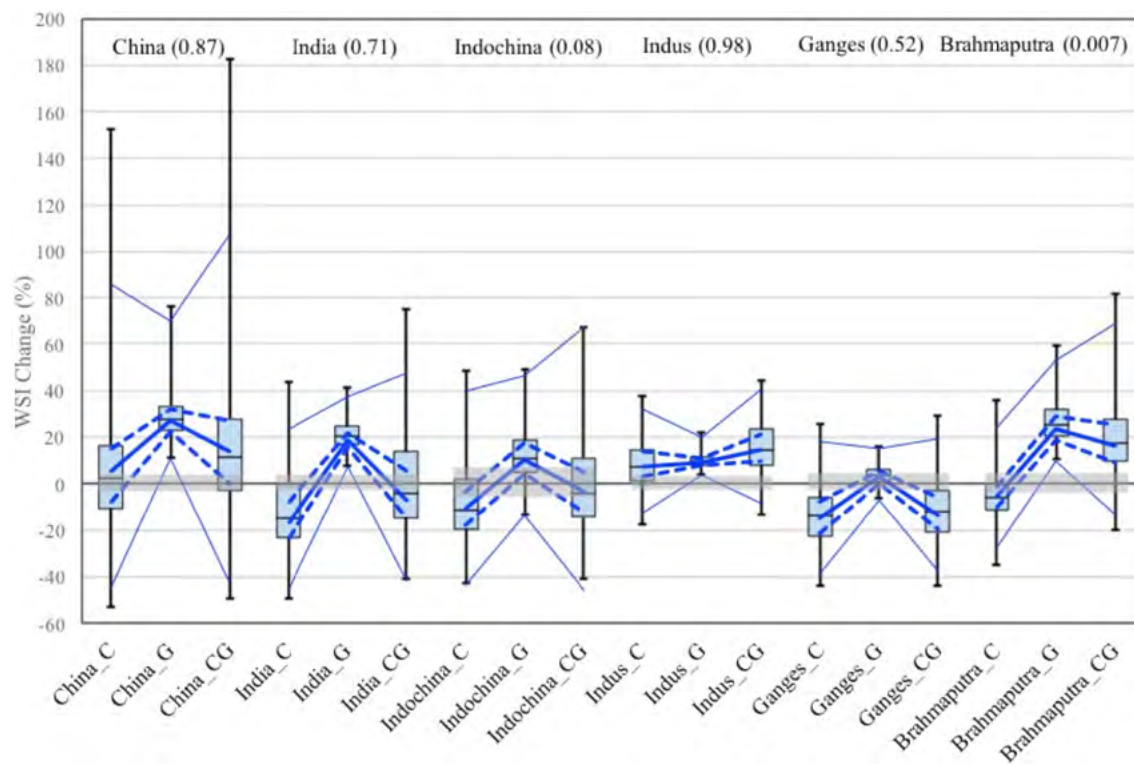


**Figure 3.** The relative changes in population-weighted water stress index, WSI (unitless) in the major regions and basins under the climate scenario ("C"), growth scenario ("G"), as well as climate and growth scenario ("CG") as a result of unconstrained emissions (whisker bar) and a stabilization policy (blue lines). The solid, dash, and dotted blue lines represent median, Q1 and Q3, minimum and maximum values, respectively. The baseline WSI values are shown at the top for each region and basin. Horizontal gray bars represent  $\pm 1$  standard deviation-equivalent relative change of population-weighted baseline WSI from 500 bootstrap samples.

population of each ASR for three impact scenarios and two policy scenarios. Also shown is  $\pm 1$  standard deviation-equivalent relative change of population-weighted baseline WSI calculated from 500 bootstrap samples (gray bar). This spread across the bootstrap ensemble can be viewed as "noise" in WSI resulting from the natural climate variability so that only changes beyond can be perceived as the actual impacts from any exterior factor. The principal cause of decreasing water stress is the greater water availability due to increased runoff related to climate change, while that of increased water stress is growing water withdrawals from varying sectors (agriculture, domestic and industry). Immediately evident is that the socioeconomic growth ("G" scenario) generally increases water stress across all the examined regions and basins under both policy scenarios. The decreased water stress exhibited by a small number of ensemble members in Indochina and the Ganges Basin is mainly attributed to the projected decreased population or slower population growth over certain ASR(s) of higher WSI values relative to other ASRs within the same region/basin. The largest median relative increase in WSI occurs in China (27%), while the smallest increase occurs in the Ganges Basin (3%). The projections are subject to a spread across the ensemble, particularly in China with increase

of 10% to 75%, Indochina, and Brahmaputra. Overall, mitigation effect is rather weak with a marginal effect on slightly lowering water stress in India and Brahmaputra. These features resonate strongly with what is observed for the changes in the domestic and industrial water withdrawals (**Figure 4**). All the examined regions and basins experience at least 40% at the 10<sup>th</sup> percentile to two- or three-fold increases in water demands at the 90<sup>th</sup> percentile, highlighting the effects of extensive growth anticipated for these developing regions and basins. The Ganges Basin shows the least relative increase in water demands, while Brahmaputra experiences the largest increase. The majority of the ASRs in India and the aggregated ASRs exhibit larger relative increases than those in China, mostly attributed to its projected higher population growth rate. This is in contrast to their projected growth-induced WSI changes, which is likely associated with the complex interplay between water demands and supply within the individual ASR and the population weighting applied when aggregating WSI to the regional level. In India, one ASR (LUN\_IND in the Indus Basin) features particularly large (about 3 to 6 fold) increase in this demand, while the ASRs in northern (Ganges river) and eastern India generally demonstrate small increases. In China, most of the ASRs in northern China

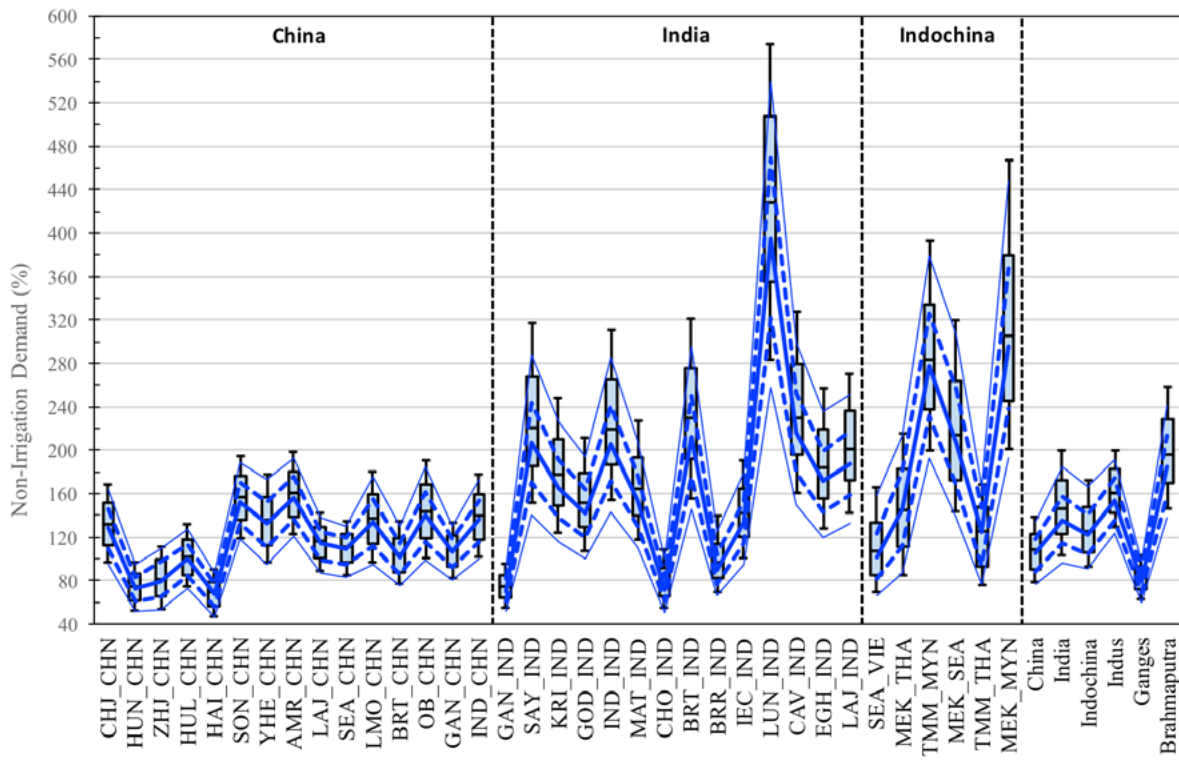


**Figure 4.** Relative change of non-irrigation demand for individual ASRs and aggregated across ASRs in major political regions and basins as a result of unconstrained emissions (whisker bar) and a stabilization policy (blue lines). The solid, dash, and dotted blue lines represent median, Q1 and Q3, 10<sup>th</sup> and 90<sup>th</sup> percentiles, respectively. We don't show minimum and maximum because of too large range.

demonstrate large relative increases. In absolute terms, these demands are, however, small in comparison with irrigation demand because their baseline values are one or two orders of magnitude smaller than the irrigation counterparts (**Figure 5**). The effect of slower growth in GDP under the L2S scenario provides a marginal buffering of such increases, particularly for the largest increase (i.e. 90<sup>th</sup> percentiles) across various ASRs in India.

Climate change alone (“C” scenario) produces a mixture of responses with both positive (decrease) and negative (increase) effects on water stress (Figure 3 and **Table 1**). In China and Indus, which are already heavily stressed under contemporary conditions, climate change presents very limited beneficial effect, with the majority of the ensembles indicating increased water stress. Especially in the Indus River, the median relative increase in WSI is nearly as strong as that resulting from socioeconomic growth. Very contrasting features can be observed over other regions or basins. Under contemporary conditions, India and the Ganges Basin are heavily and moderately stressed, respectively, while Indochina and Brahmaputra do not experience much water stress. Nevertheless, climate change has apparent beneficial effects for these regions and basins with the majority of the ensembles indicating decreased water stress. The combined effect of socioeconomic growth and climate change (“CG” scenario) is dependent on how

the two interact non-linearly, and such interplay is highly region or basin specific (Figure 3 and Table 1). In general, the negative effect of socioeconomic growth exacerbates the negative effect or offsets the positive effect of climate change, and the resulting distributions of WSI changes under the “CG” scenario tend to shift toward the higher values than under the “C” scenario. The counteracting effect of growth is particularly strong for Brahmaputra, but fairly weak for Ganges and lies in between for other regions. The resulting combined climate-growth effect on water stress remains strongly negative in China and Indus, becomes negative in Brahmaputra (the trend is reversed in sign), but retains largely positive in other three regions as climate seems able to buffer the increase in water stress imposed by economic growth. Note that the Indus Basin is the only region showing the stronger median WSI increase from climate and growth than that from growth only.

We find that the influence of climate change on water stress exhibits much larger uncertainty than economic growth. Forcing by different regional climate patterns yields the interquartile range (IQR) and total spread of WSI changes across the ensemble that are almost doubled or tripled those owing to different economic growth projections across various regions. This implies that the greatest risks to regions facing future water stress may essentially arise from regional extremes occurring with-

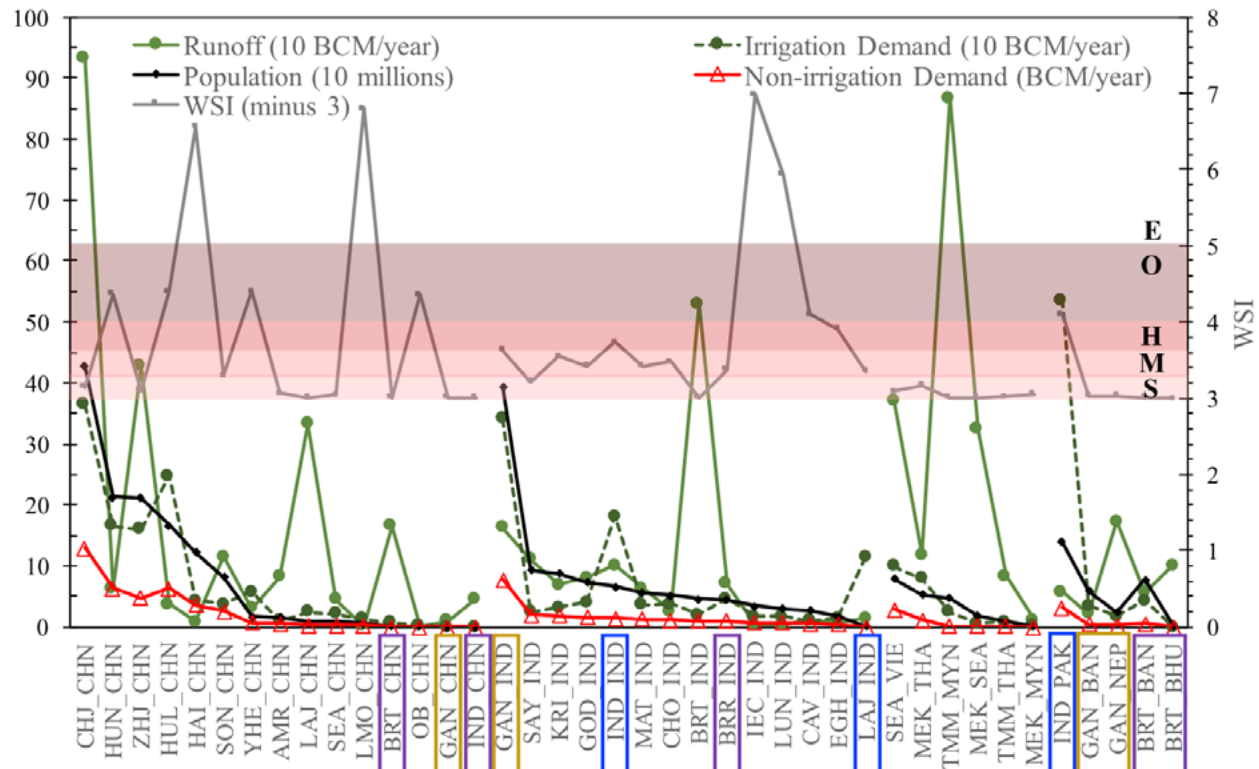


**Figure 5.** Baseline population, runoff, irrigation demand, non-irrigation demand, and WSI for individual ASRs in China (\_CHN), India (\_IND), Indochina, and part of ASRs in Indus, Ganges, and Brahmaputra. The sequence of ASRs in China, India, and Indochina is arranged in order of decreasing population. The horizontal color bars denote the water stress categories with S, M, H, O, E representing slightly, moderately, heavily, overly, and extremely, respectively. The basins in the blue, yellow, and purple rectangles represent the ASRs in Indus, Ganges, and Brahmaputra, respectively.

**Table 1.** Accumulated relative frequency of decreased and increased (the numbers in the parenthesis) population-weighted WSI, with the relative change of population-weighted baseline WSI from natural climate variability taken into account, for the major political regions and basins under three impact scenarios and two policy scenarios. Blue and red colors represent collective negative and positive effects, respectively, if accumulated relative frequency of decreased water stress is smaller than or larger than accumulated relative frequency of increased water stress. \* indicates the regions or basins consistently show increased water stress across all the scenario cases. Bold numbers indicate there are apparent mitigation impacts on reducing water stress in the regions or basins across different impact scenarios through increasing accumulated relative frequency of decreased WSI or decreasing accumulated relative frequency of increased WSI, or both.

	UE_C	UE_G	UE(CG)	L2S_C	L2S_G	L2S(CG)
China*	40% (49%)	0% (100%)	25% (64%)	32% (56%)	0% (100%)	18% (70%)
India	<b>*72%</b> (21%)	<b>**0%</b> (100%)	<b>*52%</b> (40%)	<b>82%</b> (11%)	<b>**0%</b> (100%)	<b>61%</b> (29%)
Indochina	<b>*62%</b> (18%)	<b>**2%</b> (73%)	<b>*44%</b> (32%)	<b>67%</b> (9%)	<b>**2%</b> (70%)	<b>44%</b> (23%)
Indus*	<b>**14%</b> (73%)	<b>**0%</b> (100%)	<b>**3%</b> (89%)	<b>**8%</b> (77%)	<b>**0%</b> (100%)	<b>**1%</b> (92%)
Ganges	<b>*80%</b> (10%)	<b>**4%</b> (55%)	<b>*74%</b> (15%)	<b>*85%</b> (6%)	<b>**6%</b> (47%)	<b>*80%</b> (7%)
Brahmaputra	<b>*61%</b> (18%)	<b>**0%</b> (100%)	<b>**5%</b> (86%)	<b>*59%</b> (13%)	<b>**0%</b> (100%)	<b>**4%</b> (89%)

in a subset of climate model projections. China presents the largest inter-ensemble disagreement in the magnitude of the climate-induced WSI changes, ranging from a decrease of 50% to an increase of 150%, while the counterparts over other regions are mostly constrained within  $\pm 50\%$ . The combined climate-growth effects on water stress seem largely dominated by that of uncertain regional climate change with the slightly large but similar ensemble spread. The lower water stress via a stabilization policy can

be observed for both “C” and “CG” scenarios across all the regions, by reducing distribution variance and in particular removing the extremely large WSI increases seen in the no-policy scenario (Figure 3). The stabilization policy also manifests the increased accumulative relative frequency of decreased WSI, the decreased accumulative relative frequency of increased WSI, or both (Table 1). Overall, the choice of the climate policy scenario (UE or L2S) has a much smaller effect compared with the choice of the re-

gional climate pattern trends or the choice of economic growth parameters. In consideration of all sources of uncertainty, regional climate change uncertainty is the most influential factor in water stress trends. However, it is important to note that, because of the influence of emissions before 2000 and climate inertia, the relative importance of the policy choice is expected to be greater if the simulation were extended to decades beyond 2050.

The effects of trends in climate on water stress resonate strongly with the regional features of two main drivers—runoff and irrigation demand (**Figure 6a, b**). Under contemporary conditions, we see that heavily to extremely stressed ASRs are aligned across the regions of low runoff and arid conditions (Figure 5). Substantial stress is observed in several densely-populated ASRs in the northern part of China (HUN\_CHN, HAI\_CHN, and

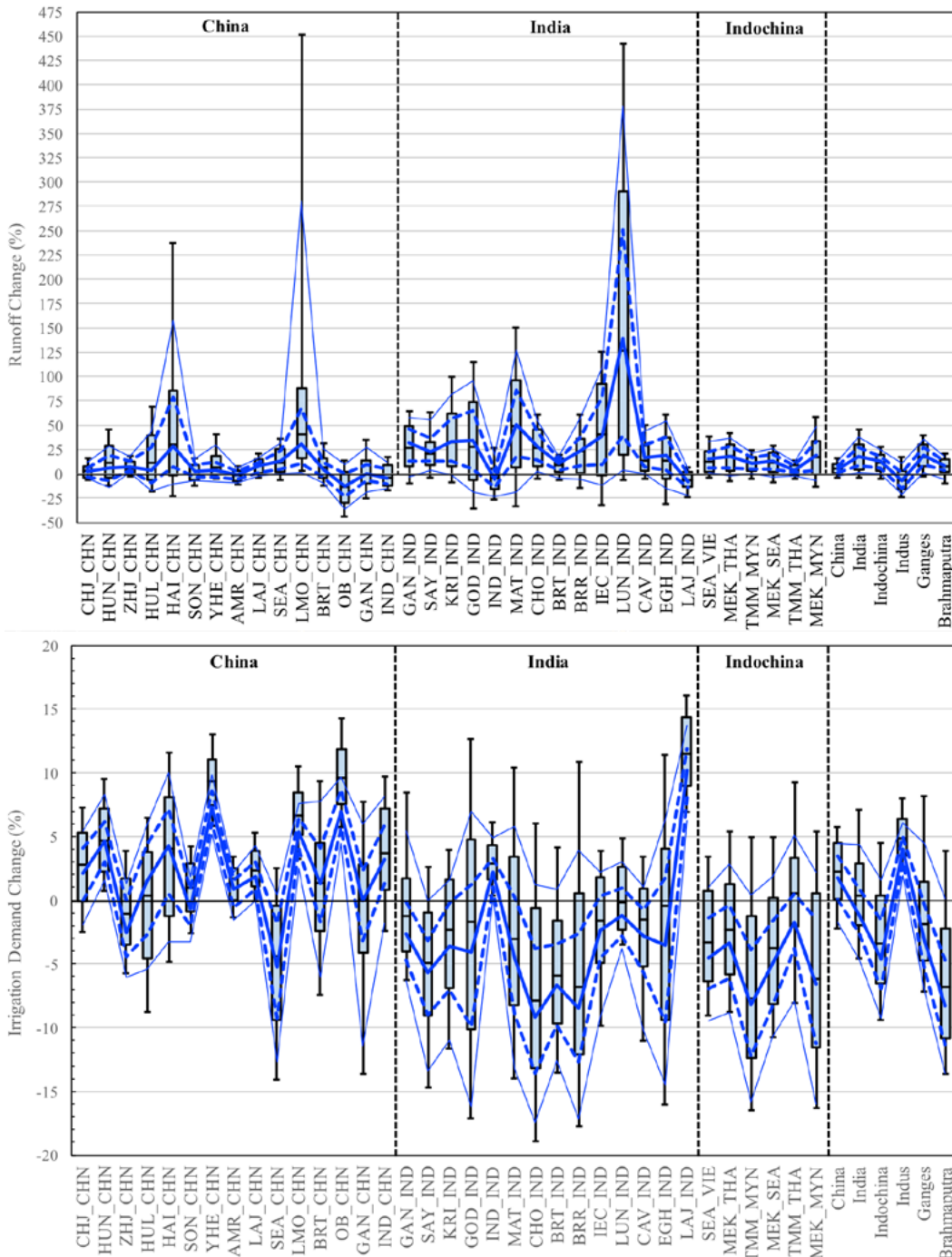


**Figure 6.** Same as Figure 4, but for a) runoff and b) irrigation demand, respectively.

HUL\_CHN), a few ASRs in northwest China (LMO\_CHN, YHE\_CHN, and OB\_CHN), and Southern India. Exceptions to this characterization are observed for ASRs located in India and Pakistan, namely GAN\_IND, IND\_IND, and IND\_PAK, showing relatively large runoff but heavily or overly exploited water resources. This is a result of the combined effects of large population and high irrigation demand.

The runoff is projected to increase in the majority of ASRs in China, India, and Indochina (Figure 6a), and to decrease in the far west and the north including Afghanistan, Pakistan, and Mongolia (not shown). In these regions, there is a relatively high level of agreement on the sign of change across the ensemble (more than 50% or 75%). Most of these large-scale features are consistent with previous studies (Haddeland *et al.*, 2014; Schewe *et al.*, 2014). In two ASRs in India (IND\_IND and LAJ\_IND) that are part of the Indus river basin, the majority of ensemble presents evident decreases. Except for the Indus Basin with a drying trend, all the other regions and basins exhibit wetting trends, with India and Ganges showing the largest relative increases and China the smallest. It is worth noting that LUN\_IND, which is one of the two extremely stressed ASRs in India and characteristic of the largest increase in the domestic and industrial water withdrawals, also demonstrates the largest uncertainty in the projected runoff change with a decrease of 6% at the 10<sup>th</sup> percentile to an increase of 440% at the 90<sup>th</sup> percentile and an IQR of 20% to 290% increase. LMO\_CHN in China also features a similarly wide range of runoff change, but its IQR is much reduced (20% to 90% increase). LMO\_CHN and HAI\_CHN show larger relative increases in runoff than other ASRs in China. The increases in water availability over these ASRs in China and India are encouraging given their extreme water stress conditions in the contemporary climate. Mitigation reduces the spread across the ensemble by weakening the extreme decreases (i.e. 10<sup>th</sup> percentile) and in particular extreme increases (i.e. 90<sup>th</sup> percentiles).

Irrigation demand features a substantially smaller relative change (-20% to 15%) than domestic and industrial demands, but from a much higher base level at present (Figure 5), so the absolute water consumption used for irrigation is the largest. The principal causes of growing agricultural withdrawals are warmer and drier conditions, which enhance the evapotranspiration of crops. Projected changes in irrigation demand thus correspond with the changes in runoff to some extent. There exists a wide disagreement on the sign of projected changes in irrigation demand across the ASRs (Figure 6b). In India, more than 90% of ensemble indicates increased demands over two ASRs of the Indus river basin (IND\_IND and LAJ\_IND), while the majority of the ensemble (more

than 50% or 75%) suggests decreased demands over the other ASRs. In China, except for two ASRs in southern China (SEA\_CHN and ZHJ\_CHN) that are dominated by decreased demands, all the other ASRs tend to have increased demands. In particular, all the ensemble of the ASRs in northwestern China (YHE\_CHN, LMO\_CHN, OB\_CHN) as well as more than 90% of the ensemble of the Yellow river (HUN\_CHN) consistently suggests increased irrigation consumption. Such a high level of consistency in the sign of change indicates high confidence. In the Indochina region, climate change favors reduced irrigation demands across all the ASRs. For a regional or basin-scale aggregate, we see that the Indus Basin and China are mostly governed by increased irrigation, while Indochina, Ganges, and Brahmaputra are largely dominated by decreased irrigation. There is no clear trend in India, with the median of the ensemble slightly favoring increased irrigation. Likewise, mitigation tends to reduce the distribution variance by weakening extreme increases and decreases in irrigation consumption. This can be observed across all the ASRs.

Given these considerations, the positive climate-driven effects on water stress in India, Indochina, Ganges, and Brahmaputra mostly benefit from increased runoff and decreased irrigation demands, while the negative effect of climate change in the Indus Basin is mostly attributed to decreased runoff and increased irrigation demands. Although there exist ubiquitous runoff increases across most China ASRs, increases in irrigation demand are the main contributor to changes in water stress, leading to the negative climate effect.

### 3.2 Population at Risk to Water Stress

We further assess the population that is prone to water-stress exposure under current conditions and future scenarios by assigning the WSI of each ASR to one of the water stress classifications. All ASRs with WSI values larger than 0.6 (the heavily to extremely exploited category) are deemed as exposed to “water stress” and tabulated according to their population. These tabulations are performed for all the ensembles of each of the 6 future scenarios. The populations under water stress were derived based on the collective percentage across the ensemble and aggregated by all ASRs and ASRs of each region (**Table 2**).

Overall, the increases in population exposed to water-stressed conditions as a result of socioeconomic growth is the same order of magnitude as any change in the climate-only scenarios. In China and Indus, regardless of the effect of socioeconomic growth or climate change or their combination, additional population at risk of exposure to at least a heavy level of water stress is approximately 80 and 150 million, equivalent to 40% and 100%

**Table 2.** Changes in total population (parenthesis of 3<sup>rd</sup> column) and population exposed to water stress (in million) for major political regions and basins under three impact scenarios and two policy scenarios. The total population of 2041–2050 is the average from 400-ensemble projections. Bold numbers indicate decreases in population.

Area	Population		Population Exposed to Water Stress (WSI > 0.6)							
	2000	2041–2050	2000	2041–2050 (changes relative to 2000)						
				UE_C	UE_G	UE(CG)	L2S_C	L2S_G	L2S(CG)	
China	1278	1480 (202)		524	80	83	81	83	83	
India	1018	1555 (537)		567	<b>-96</b>	449	<b>-11</b>	<b>-143</b>	443	<b>-73</b>
Indochina	204	350 (146)		0	0	0	0	0	0	
Indus	206	357 (151)		205	138	151	147	146	151	150
Ganges	477	752 (275)		395	<b>-216</b>	208	<b>-187</b>	<b>-254</b>	208	<b>-224</b>
Brahmaputra	126	217 (91)		0	0	0	0	0	0	
Asia	2930	4144 (1214)		1241	143	657	195	104	651	135

of their projected population increases, respectively. The resulting total population-under-stress, by 2050, could reach 600 and 350 million, respectively. We find that most of these population are exposed to overly to extremely exploited conditions (Figure 7c, d), indicating that water requirements will consistently exceed the managed surface water supply. Although China presents an environment that is posed for expansive increase in water stress, the population-under-stress increases are somewhat limited relative to Indus. Not only is China's population increase small compared with Indus (16% versus 73%), but also a large portion of its population (about 60%) in ASRs currently experience only slightly water-stressed conditions (Figure 5), such as the Zhujiang (ZHI\_CHN) and Yangtze (CHJ\_CHN) basins across southern China. All population in the Indus Basin currently experience at least heavily water-stressed conditions with two-thirds exposed to overly exploited conditions. Stabilization does very little to reduce the population under water stress in these areas.

In contrast, socioeconomic growth shows a large effect on increasing risks to water stress in India and Ganges where the population experiences relatively large increases (~50%). In these regions, the population-under-stress by 2050 as a result of socioeconomic growth are nearly double the current estimates, representing an increase of 450 and 200 million people, respectively. Most of these population are exposed to heavily exploited conditions (Figure 7b, Ganges not shown), indicating that the managed surface water supply is under pressure but still sufficient for consumptive use. Climate-only scenarios show substantial reduction in population under water stress from the year 2000, mostly

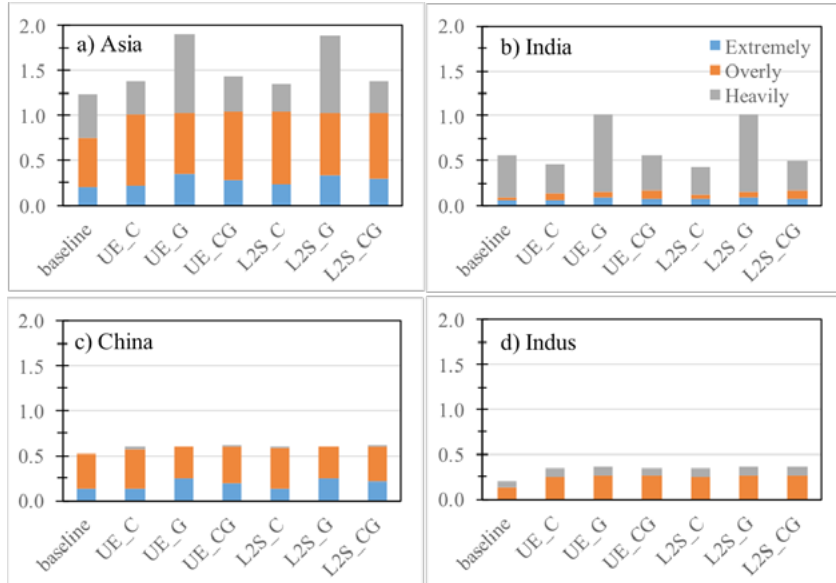


**Figure 7.** Population (in billions) exposed to three severity levels of water stress.

notable for the stabilization scenario—which can reduce the population-under-stress by approximately 150 and 250 million for India and Ganges, respectively, as compared to 100 and 200 million without climate policy. The decreases in WSI from climate change seem large enough to diminish the water-stressed conditions and reverse the substantial increases in population-under-stress represented by the socioeconomic growth. The combined effects of socioeconomic growth and climate change result in notable net decreases in population-under-stress from the contemporary condition, especially in the stabilization scenario.

In Brahmaputra and Indochina, the contemporary water stress estimate shows that all ASRs in these regions are experiencing only slight water-stressed conditions. Despite the large population increases (70%) that contribute to the substantial growth in nonagricultural water demands (Figure 4), increases in water stress seem not large enough for these regions to be moved into the wa-

ter-stressed categories. In combination with increased runoff and decreased irrigation consumption (Figure 6a, b), the total population projected to live in these regions will not be exposed to water stress across all scenarios.

In the entire study region, all the scenarios suggest increases in water-stressed population, with socioeconomic growth leading to larger increases (650 million) than climate change (150 million) and combined climate-growth effects (200 million). The socioeconomic growth increases population-under-stress across all three categories with most of the increases, in absolute terms, occurring in heavily exploited condition. Under the “C” and “CG” scenarios, increases in water-stressed population occur mostly in overly exploited conditions, while decreases occur under heavily exploited conditions. Stabilization clearly helps reduce climate change induced increases in population-under-stress.

#### 4. Summary and Discussion

The consistent, integrated modeling framework presented here employs large ensembles that capture the spectrum of regional climate response, range of economic

projections, and possible climate policies to identify where and what level of water risks may emerge and the underlying causes of potential increased stresses in Southern and Eastern Asia. The results reveal that water stress changes are far more responsive to climate drivers than to socioeconomic growth. Climate mitigation alone can help to a certain extent, particularly by reducing extreme increases in water stress, but is not sufficient to curtail all risks of increasing water scarcity by midcentury, particularly in China and Indus. To make salient risk reductions by 2050, broad adaptive measures need to be considered that increase the efficiency of water consumption as well as viable options to increase water-storage potential. A combination of both approaches may be the most effective to combat the climate problem.

There are a number of key issues associated with the development of appropriate indicators to assess water system risks, including the definition of an appropriate indicator of pressure on water resources and the specification of critical thresholds for water resource stresses. The use of different indicators could lead to a different quantification of the change in the amount of available resources

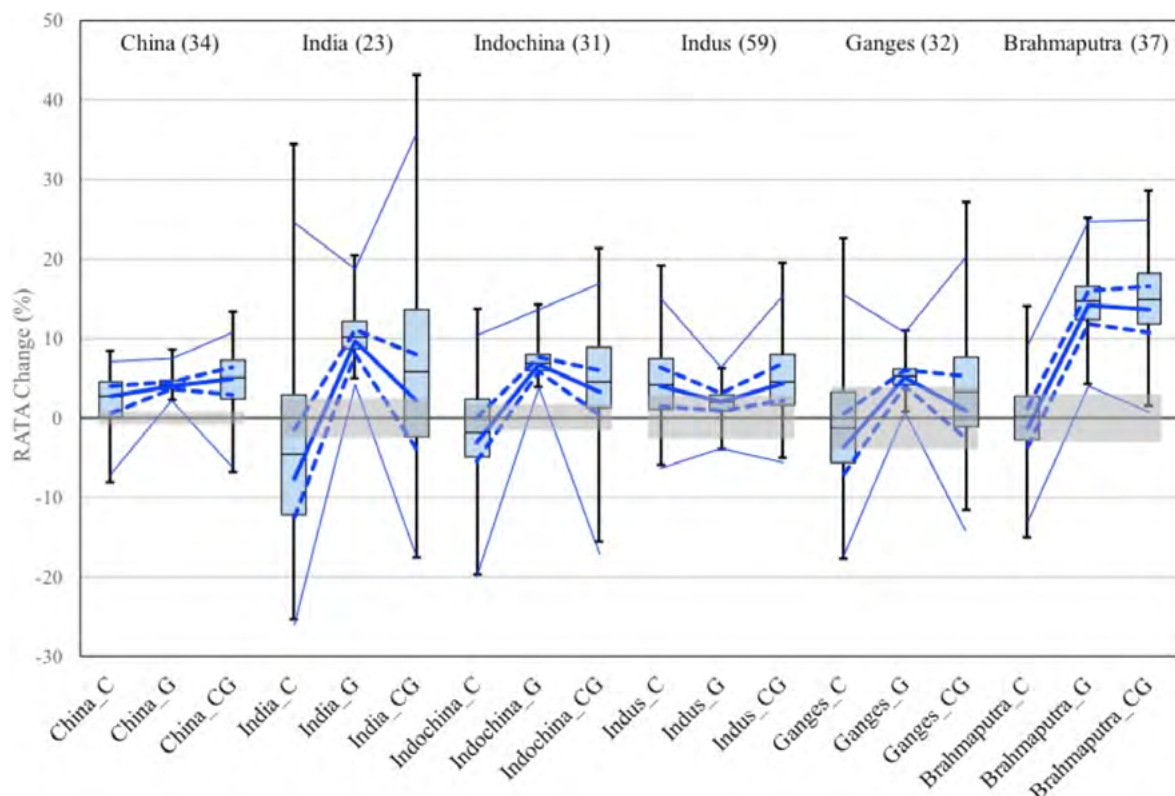


**Figure 8.** The relative changes in population-weighted Unmet Water Requirement (UWR) in the major regions and basins under the climate scenario (“C”), growth scenario (“G”), as well as climate and growth scenario (“CG”) as a result of unconstrained emissions (whisker bar) and a stabilization policy (blue lines). UWR is the percentage of the total water requirement that is not met by the system. In WRS model, total water requirement is an estimate of the amount of water that would be consumed given socioeconomic factors, climate conditions, and current infrastructure if water is an unlimited resource. The solid, dash, and dotted blue lines represent median, Q1 and Q3, minimum and maximum values, respectively. The baseline UWR values (in percentage) are shown at the top for each region and basin. Horizontal gray bars represent  $\pm 1$  standard deviation-equivalent relative change of population-weighted baseline UWR from 500 bootstrap samples.

and the resulting water resource stress. In comparison with WSI, the use of Unmet Water Requirement (UWR) as a measure of water stress, which is the percentage of the total water requirement that is not met by the system, shows apparent inconsistencies (**Figure 8**). Not only the combined climate-growth effects stay strongly negative across all the examined regions, but also, India presents the largest inter-ensemble disagreement in the magnitude of the climate-induced WSI changes while China presents the smallest. Additionally, caveats could arise from the use of threshold-based indicators of water stress because small changes in indicator value can push some large and populous watersheds from one side of the threshold to the other and therefore largely change the number of people under the specific water-stressed category.

For more rigorous assessment of future risks to water systems, several features we have not explored yet must be noted—for example, adjustments in irrigated acreage or in cropping patterns and uncertain or alternative

population projections. Additionally, a study found that hydrological models, which are responsible for translating uncertain climate model projections into changes in hydrological variables such as surface or subsurface runoff and river discharge, may contribute considerably in many regions to the uncertainty in water resource projections (Schewe *et al.*, 2014). Efforts are needed to represent this additional level of uncertainty. Nevertheless, this model framework is easily integrated with new features and applied to other specific areas of interest, and further provides persuasive and actionable insights for strategic planning and risk management in the face of both unavoidable and preventable global change.

### Acknowledgements

This work was supported by the Department of Energy under An Integrated Framework for Climate Change Assessment (DE-FG02-94ER61937) and other government, industry and foundation sponsors of the MIT Joint Program on the Science and Policy of Global Change. For a complete list of sponsors and U.S. government funding sources, see <http://globalchange.mit.edu/sponsors>.

## 5. References

- Alcamo, J., M. Flörke and M. Märker (2007): Future long-term changes in global water resources driven by socio-economic and climatic changes. *Hydrolog. Sci. J.* **52**: 247–275.
- Arndt, C. *et al.* (2015): Informed selection of future climate. *Clim. Chang.* **130**: 21–33.
- Arnell, N.W. (2004): Climate change and global water resources: SRES emissions and socio-economic scenarios. *Glob. Environ. Chang.* **14**: 31–52.
- Chellanay, B. (2012): Asia's worsening water crisis. *Survival* **54**: 143–156.
- Fant, C. *et al.* (2012): CliCrop: A crop water-stress and irrigation demand model for an integrated global assessment modeling approach. *MIT JSPGC Report 214*, April, 26 p.
- Fant, C. *et al.* (2016): Projections of water stress based on an ensemble of socioeconomic growth and climate change scenarios: A case study in Asia. *PLoS ONE* **11**(3): e0150633.
- Haddeland, I. *et al.* (2014): Global water resources affected by human interventions and climate change. *Proc. Natl. Acad. Sci. USA* **111**: 3251–3256.
- Hagemann, S. *et al.* (2013): Climate change impact on available water resources obtained using multiple global climate and hydrology models. *Earth Syst. Dynam.* **4**:129–144.
- Lall, U., and A. Sharma (1996): A nearest neighbor bootstrap for resampling hydrologic time series. *Water Resour. Res.* **32**: 679–693.
- Meehl, G.A. *et al.* (2007): The WCRP CMIP3 multi-model dataset: A new era in climate change research. *Bull. Am. Meteorol. Soc.* **88**: 1383–1394.
- Oleson, K.W. *et al.* (2004): Technical description of the Community Land Model (CLM). National Center for Atmospheric Research, *Tech. Note NCAR/TN-461+STR*, 173 pp.
- Paltsev, S. *et al.* (2004): The MIT Emissions Prediction and Policy Analysis (EPPA) Model: Version 4. *MIT JSPGC Report 125*, August, 72 p.
- Population Reference Bureau (2015): *2015 World Population Data Sheet*. Population Reference Bureau, Washington, DC, USA ([http://www.prb.org/pdf15/2015-world-population-data-sheet\\_eng.pdf](http://www.prb.org/pdf15/2015-world-population-data-sheet_eng.pdf))
- Ramirez-Villegas, J., and A. Jarvis (2010): Downscaling global circulation model outputs: the delta method decision and policy analysis working paper No. 1. International Center for Tropical Agriculture (CIAT), Cali, Colombia.
- Rosegrant, M. *et al.* (2008): International Model for Policy Analysis of Agricultural Commodities and Trade (IMPACT): Model Description. International Food Research Institute, Washington, D.C.
- Schewe, J. *et al.* (2014): Multimodel assessment of water scarcity under climate change. *Proc. Natl. Acad. Sci. USA* **111**: 3245–3250.
- Schlosser, C.A. *et al.* (2012): Quantifying the likelihood of regional climate change: A hybridized approach. *J. Clim.* **26**: 3394–3414.
- Schlosser, C.A. *et al.* (2014): The future of global water stress: An integrated assessment. *Earth's Future* **2**: 341–361.
- Sheffield, J., G. Goteti and E.F. Wood (2006): Development of a 50-year high-resolution global dataset of meteorological forcings for land surface modeling. *J. Climate* **19**: 3088–3111.
- Siegfried, T. *et al.* (2011): Will climate change exacerbate water stress in Central Asia? *Clim. Chang.* **112**: 881–899.
- Smakhtin V., C. Revanga and P. Doll (2005): Taking into account environmental water requirements in global scale water resources assessments, 2005. (<http://www.iwmi.cgiar.org/assessment/files/pdf/publications/researchreports/carr2.pdf>).
- Strzepek, K. *et al.* (2013): Modeling water resource systems under climate change: IGSM-WRS. *J. Adv. Earth Model Sys.* **5**: 638–653.
- UN-Water (2007): Coping with water scarcity: challenge of the twenty-first century. (<http://www.fao.org/3/a-aq44e.pdf>).
- Vörösmarty, C.J., P. Green, J. Salisbury, and R.B. Lammers (2000): Global water resources: Vulnerability from climate change and population growth. *Science* **289**: 284–288.
- Webster, M.D. *et al.* (2012): Analysis of climate policy targets under uncertainty. *Clim. Chang.* **112**: 569–583.

# Joint Program Report Series - Recent Articles

For limited quantities, Joint Program Reports are available free of charge. Contact the Joint Program Office to order.

Complete list: <http://globalchange.mit.edu/publications>

315. The Future Water Risks Under Global Change in Southern and Eastern Asia: Implications of Mitigation. *Gao et al., Jul 2017*
314. Modeling the Income Dependence of Household Energy Consumption and its Implications for Climate Policy in China. *Caron et al., Jul 2017*
313. Global economic growth and agricultural land conversion under uncertain productivity improvements in agriculture. *Lanz et al., Jun 2017*
312. Can Tariffs be Used to Enforce Paris Climate Commitments? *Winchester, Jun 2017*
311. A Review of and Perspectives on Global Change Modeling for Northern Eurasia. *Monier et al., May 2017*
310. The Future of Coal in China. *Zhang et al., Apr 2017*
309. Climate Stabilization at 2°C and Net Zero Carbon Emissions. *Sokolov et al., Mar 2017*
308. Transparency in the Paris Agreement. *Jacoby et al., Feb 2017*
307. Economic Projection with Non-homothetic Preferences: The Performance and Application of a CDE Demand System. *Chen, Dec 2016*
306. A Drought Indicator based on Ecosystem Responses to Water Availability: The Normalized Ecosystem Drought Index. *Chang et al., Nov 2016*
305. Is Current Irrigation Sustainable in the United States? An Integrated Assessment of Climate Change Impact on Water Resources and Irrigated Crop Yields. *Blanc et al., Nov 2016*
304. The Impact of Oil Prices on Bioenergy, Emissions and Land Use. *Winchester & Ledvina, Oct 2016*
303. Scaling Compliance with Coverage? Firm-level Performance in China's Industrial Energy Conservation Program. *Karplus et al., Oct 2016*
302. 21<sup>st</sup> Century Changes in U.S. Heavy Precipitation Frequency Based on Resolved Atmospheric Patterns. *Gao et al., Oct 2016*
301. Combining Price and Quantity Controls under Partitioned Environmental Regulation. *Abrell & Rausch, Jul 2016*
300. The Impact of Water Scarcity on Food, Bioenergy and Deforestation. *Winchester et al., Jul 2016*
299. The Impact of Coordinated Policies on Air Pollution Emissions from Road Transportation in China. *Kishimoto et al., Jun 2016*
298. Modeling Regional Carbon Dioxide Flux over California using the WRF-ACASA Coupled Model. *Xu et al., Jun 2016*
297. Electricity Investments under Technology Cost Uncertainty and Stochastic Technological Learning. *Morris et al., May 2016*
296. Statistical Emulators of Maize, Rice, Soybean and Wheat Yields from Global Gridded Crop Models. *Blanc, May 2016*
295. Are Land-use Emissions Scalable with Increasing Corn Ethanol Mandates in the United States? *Ejaz et al., Apr 2016*
294. The Future of Natural Gas in China: Effects of Pricing Reform and Climate Policy. *Zhang & Paltsev, Mar 2016*
293. Uncertainty in Future Agro-Climate Projections in the United States and Benefits of Greenhouse Gas Mitigation. *Monier et al., Mar 2016*
292. Costs of Climate Mitigation Policies. *Chen et al., Mar 2016*
291. Scenarios of Global Change: Integrated Assessment of Climate Impacts. *Paltsev et al., Feb 2016*
290. Modeling Uncertainty in Climate Change: A Multi-Model Comparison. *Gillingham et al., Dec 2015*
289. The Impact of Climate Policy on Carbon Capture and Storage Deployment in China. *Zhang et al., Dec 2015*
288. The Influence of Gas-to-Liquids and Natural Gas Production Technology Penetration on the Crude Oil-Natural Gas Price Relationship. *Ramberg et al., Dec 2015*
287. Impact of Canopy Representations on Regional Modeling of Evapotranspiration using the WRF-ACASA Coupled Model. *Xu et al., Dec 2015*
286. Launching a New Climate Regime. *Jacoby & Chen, Nov 2015*
285. US Major Crops' Uncertain Climate Change Risks and Greenhouse Gas Mitigation Benefits. *Sue Wing et al., Oct 2015*
284. Capturing Natural Resource Dynamics in Top-Down Energy-Economic Equilibrium Models. *Zhang et al., Oct 2015*
283. Global population growth, technology, and Malthusian constraints: A quantitative growth theoretic perspective. *Lanz et al., Oct 2015*
282. Natural Gas Pricing Reform in China: Getting Closer to a Market System? *Paltsev & Zhang, Jul 2015*
281. Impacts of CO<sub>2</sub> Mandates for New Cars in the European Union. *Paltsev et al., May 2015*
280. Water Body Temperature Model for Assessing Climate Change Impacts on Thermal Cooling. *Strzepek et al., May 2015*
279. Emulating maize yields from global gridded crop models using statistical estimates. *Blanc & Sultan, Mar 2015*